Journal of Photochemistry and Photobiology A: Chemistry 198 (2008) 75–84

Contents lists available at ScienceDirect

Journal of Photochemistry and Photobiology A: Chemistry

journal homepage: www.elsevier.com/locate/jphotochem

Dynamic quenching of porphyrin triplet states by two-photon absorbing dyes: Towards two-photon-enhanced oxygen nanosensors

Olga S. Finikova[a], Ping Chen[b], Zhongping Ou[b], Karl M. Kadish[b], Sergei A. Vinogradov[a,*]

[a] Department of Biochemistry and Biophysics, University of Pennsylvania, Philadelphia, PA 19104, United States
[b] Department of Chemistry, University of Houston, Houston, TX 77204, United States

ARTICLE INFO

Article history:
Received 31 December 2007
Received in revised form 13 February 2008
Accepted 25 February 2008
Available online 29 February 2008

Keywords:
Phosphorescence
Oxygen
Porphyrin
Two-photon
Electron transfer

ABSTRACT

Two-photon-enhanced dendritic nanoprobes are being developed for two-photon (2P) laser scanning microscopy of oxygen [R.P. Briñas, T. Troxler, R.M. Hochstrasser, S.A. Vinogradov, J. Am. Chem. Soc. 127 (2005) 11851–11862]. In these molecular constructs, phosphorescence of metalloporphyrins is coupled to two-photon absorption (2PA) of electronically separate antenna dyes *via* intramolecular Förster-type resonance energy transfer (FRET). In the originally developed probes, competing electron transfer (ET) between the antennae and the long-lived triplet states of metalloporphyrins partially quenched the phosphorescence, reducing the probe's sensitivity and dynamic range. The rate of such ET can be reduced by tuning the redox potentials of the chromophores. In order to identify the optimal metalloporphyrin-2P antenna pairs, we performed screening of several phosphorescent Pt porphyrins (FRET acceptors) and 2P dyes (FRET donors) using dynamic quenching of phosphorescence. Phosphorescence lifetimes of Pt porphyrins were measured as a function of the dye concentration in organic solutions. The obtained Stern–Volmer quenching constants were correlated with the corresponding ET driving forces (ΔG_{ET}), calculated using the Rehm–Weller equation. FRET pairs with minimal quenching rates were identified. The developed approach allows convenient screening of candidate-compounds for covalent assembly of 2P-enhanced triplet nanodevices. Systematic electrochemical measurements in a series of Pt porphyrins with varying peripheral substitution and conjugation pathways are presented.

1. Introduction

Molecular devices capable of generation of triplet states upon two-photon (2P) excitation have been the focus of several recent studies, including construction of 2P agents for photodynamic therapy [2–5] and 2P phosphorescent oxygen nanosensors [1,6]. Phosphorescent probes used in biological oxygen measurements [7] are based on metalloporphyrins, whose 2P absorption (2PA) cross-sections (σ_2) are very small, and their ability to generate emissive triplet states upon 2P excitation is unacceptably low for consideration in imaging applications [1,8]. 2P-enhanced phosphorescent probes make use of the Förster-type resonance energy transfer (FRET) as a coupling mechanism between the absorption by an array of 2P chromophores (2P antenna) and the excitation of a metalloporphyrin (core). The latter is followed by the intersystem crossing (isc) within the porphyrin and the emission of phosphorescence [1].

One problem inherent to the design of FRET-based 2PA phosphorescent probes is quenching of the triplet states by photoinduced electron transfer (ET), involving the metalloporphyrin and the 2P antenna [6]. Metalloporphyrin triplet states are very long-lived (tens to hundreds of microseconds), and even slow intramolecular quenching processes can be deleterious to their emission. For example, phosphorescence quantum yields of some of the earlier reported probes were reduced by as much as 50–100 times due to intramolecular ET's [1,6].

Tuning intramolecular distances between the core and the 2P antennae provides an effective mechanism for manipulating the rates of ET and FRET in order to increase the sensor performance [6]. This strategy is general and can be applied even in those cases when the ET is strongly favored thermodynamically. However, by far the most effective way to eliminate the unwanted quenching processes is to cancel their driving forces by adjusting the redox potentials of the participating chromophores.

One approach to evaluate potential 2PA antenna/phosphorecent core pairs in photoinduced ET reactions is based on dynamic quenching of phosphorescence. Dynamic quenching [9,10] of long-lived triplet states [11,12] by freely diffusing quenching species in solution is a well-known phenomenon. Practical aspects of dynamic quenching as analytical technique, e.g. for studies of protein structure and dynamics, were extensively reviewed [9,10,13,14]. In particular, quenching of excited states of aromatic molecules *via*

* Corresponding author.
E-mail address: vinograd@mail.med.upenn.edu (S.A. Vinogradov).

1010-6030/$ – see front matter © 2008 Elsevier B.V. All rights reserved.
doi:10.1016/j.jphotochem.2008.02.020

electron and energy transfer was studied in detail in 1960s–1970s, when the fundamentals of quenching kinetics were established [15–17]. Quenching by photoinduced ET [17] has been extensively researched in relation to solar energy conversion and biological photosynthetic systems [18].

In a dynamic quenching experiment, the rate of ET can be estimated by measuring the dependence of the excited state lifetime on the concentration of quencher, unless the ET rate is greater than the rate of diffusion. Dynamic quenching is especially well suited for measuring triplet quenching by the ET because of inherently high sensitivity of long phosphorescence lifetimes ($\sim 10^{-3}$ to 10^{-5} s) to the presence of quenching species in the environment [19]. In the present work we used dynamic quenching of phosphorescence to study ET reactions between sets of phosphorescent Pt porphyrins and 2P dyes in order to identify FRET pairs with minimal ET driving forces for construction of covalent 2P-enhanced nanosensors.

2. Experimental

2.1. Materials

Pt porphyrin **3** (PtTPP) was obtained from Frontier Scientific, Inc. Pt porphyrins **1**, **2**, **4**–**11** were synthesized by inserting platinum into the corresponding free bases in refluxing benzonitrile using the method proposed by Buchler et al. [20]. Non-extended free-base porphyrins for syntheses of PtP's **1**, **2**, **4**–**8** were prepared using the Lindsey method [21]. Free-base porphyrins for syntheses of PtTBP's **9**–**11** were prepared using the method developed earlier [22].

Dye **A** (AF-50) was a courtesy of Dr. L.-S. Tan (AFRL/MLBP). Dyes **C** and **D** were synthesized using the method described by Blanchard-Desce and coworkers [23] and Ulman et al. [24] with minor modifications. Dye **B** [24], dye **E** [1] and dye **F** [25] were prepared as described previously.

Detailed description of the synthetic procedures and characterization data are available in Supporting Information.

2.2. Spectroscopic and electrochemical measurements

Optical spectra were recorded on a PerkinElmer Lambda 35 UV–vis spectrophotometer. Steady-state fluorescence and phosphorescence measurements were performed on a SPEX Fluorolog-2 spectrofluorometer (Jobin-Yvon Horiba). Emission spectra were obtained using solutions with no more than 0.1 OD in the absorbance maxima. Typically, at the excitation wavelength, the absorbance of a sample was 0.05–0.06 OD. Quartz fluorometric cells (Starna, Inc., 1 cm optical path length) were used in linear optical experiments. Emission quantum yields were measured relative to the fluorescence of rhodamine B (RhB) in MeOH ($\phi_{fl} = 0.5$) [26,27]. Time resolved phosphorescence measurements were performed using an in-house constructed phosphorometer [28] modified for time-domain operation. The excitation sources in this instrument are 1 W LED's (Hewlett Packard, $\lambda_{max} = 530$ and 635 nm for excitation of PtP's and PtTBP's, respectively), whose output is controlled by a 333 kHz D/A board (MIO-16, National Instruments, Inc.).

2PA cross-sections of compounds were determined by the relative emission method, using rhodamine B in MeOH as a standard ($\lambda_{ex} = 840$ nm, $\sigma_2 \approx 210$ GM) [29,30]. 2PA measurements were conducted using a system based on a femtosecond Ti:Sapphire oscillator (Coherent Mira 900, $\lambda_{max} = 840$ nm, 110 fs, 76 MHz rep. rate). The output of the laser was passed through a half-wave plate and a polarizing cube, so that the excitation power could be adjusted continuously, and directed into the objective (Nikon FLUOR X40, 170 μm focal distance, NA 1.3) of an inverted microscope (Nikon, Diaphot 300). The power of the excitation beam was measured before it entered the microscope using an optical power meter (Molectron). The sample solution was placed in a cylindrical cuvette, one side of which was made out of a thin microscope cover slip. The emission was collected by the objective, passed through a dichroic beam splitter (Nikon 835dcsp) and a short-pass cut-off filter (sp785 nm, RazorEdge, Semrock) and directed into a monochromator (Acton SP150). The output of the monochromator was projected on a N_2-cooled CCD camera (Roper Scientific) and recorded using WinSpec32 software (Roper Scientific). The 2P origin of the absorption was confirmed in each case by plotting quadratic dependence of the emission signal on the excitation power.

The oxidation and reduction potentials were measured on a EG&G Potentiostat (Model 173) at 298 K. A three-electrode system was used, which consisted of a glassy carbon or platinum disk working electrode, a platinum wire counter electrode and a saturated calomel reference electrode (SCE). The SCE electrode was separated from the bulk of the solution by a fritted-glass bridge of low porosity that contained the solvent supporting electrolyte mixture. The solvent for the electrochemical experiments, absolute *N*,*N*-dimethylformamide (DMF, Fluka Chemical Co.), and the supporting electrolyte, tetra-*n*-butylammonium perchlorate (TBAP, Fluka Chemical Co.) were used as received without further purification. Half-wave potentials were calculated as $E_{1/2} = (E_{pa} + E_{pc})/2$ at a scan rate of 0.1 V/s and are referenced to the Fc/Fc^+ (Ferrocene >98%, Fluka Chemical Co.)

2.3. Quenching experiments

The titration cell for the dynamic quenching measurements consisted of a glass vial (vol. ~2 ml) with a polypropylene stopper, in which two stainless steel needles were inserted to provide inlet and outlet ports for Ar. The inlet needle was immersed in the solution to allow effective bubbling. Solution of a Pt porphyrin (1 ml, $OD_{512\,nm} = 0.1 \pm 0.01$) in DMF (Fisher Scientific, Inc., Biotech grade, 99.9+%) was placed inside the vial, which was positioned inside a cuvette holder shaded from the ambient light. The excitation and emission light was delivered to and from the vial by a pair of optical fibers (Ø 3 mm), positioned at the right angle with respect to one another. Phosphorescence was excited by 5-μs long pulses ($\lambda_{ex} = 530$ nm for non-extended PtP's (**1**–**8**); $\lambda_{ex} = 635$ nm for PtTBP's (**9**–**11**)), followed by 1 ms measurement period. 100–200 decays were averaged to give SNRs (signal-to-noise ratio) >100. The decays were analyzed by least-squares fitting to single-exponentials.

In a typical dynamic quenching experiment, oxygen was displaced from the solution by Ar until the phosphorescence lifetime, recorded at 10 s intervals, became constant (reached a plateau). An aliquot of a solution of 2PA dye in DMF was added, and Ar bubbling was resumed until the phosphorescence lifetime reached the next plateau. For each dye concentration (5–6 in total), the mean phosphorescence lifetime was calculated as the average across the plateau; the first plateau (no quencher added) corresponded to the native phosphorescence lifetime (τ_0). Stern–Volmer quenching plots ($1/\tau - 1/\tau_0$ *vs.* [Q]) were used to calculate the quenching constants (k_q). Each k_q value was derived as the average from three independent experiments. k_q values from different experiments varied within no more than 10% of the average.

3. Results and discussion

3.1. Approach

Under conditions of pure dynamic quenching, kinetic data are described by linear Stern–Volmer plots, which relate changes in the

luminescence lifetimes τ to the concentration of quencher [Q]:

$$\frac{\tau_0}{\tau} = 1 + \tau_0 k_q[Q] \quad (1)$$

where τ_0 is the intensity and the lifetime in the absence of quencher. The observed quenching rate constants k_q are determined by the rate-limiting step (such as diffusion or electron transfer); and the presence of a correlation between k_qs and the ET driving forces (ΔG_{ET}) in a series of similar emitter/quencher pairs suggests that the ET is the predominant quenching mechanism [31].

The triplet state of a chromophore can be either the electron donor or the acceptor, depending on the quencher used, and the ET driving force can be estimated from the ground state redox potentials and the excitation energy according to the Rehm–Weller equation [32]:

$$\Delta G_{ET} = E_{ox}(D) - E_{red}(A) - \Delta E_{00} + w \quad (2)$$

Here ΔG_{ET} is the driving force; $E_{ox}(D)$ and $E_{red}(A)$ are the reduction and the oxidation potentials of the donor and the acceptor in their ground states, respectively; ΔE_{00} is the excitation energy (donor or acceptor); and $w = w_P - w_R$ is the work term, consisting of the Coulombic energies of reactants (w_R) and products (w_P) [32]. According to (2), ΔG_{ET} will become less negative (weaker driving force) upon (i) an increase in the oxidation potential of the donor, (ii) a decrease in the reduction potential of the acceptor and (iii) a decrease in the excitation energy ΔE_{00}.

The rate of ET is related to ΔG_{ET} through the Arrhenius and Marcus equations [33], and is expected to grow exponentially with an increase in $|\Delta G_{ET}|$, assuming $\Delta G_{ET} < 0$, up until it reaches the diffusion limit [34]. Formal kinetics can be used to express the observed Stern–Volmer quenching constant in terms of the ET rate.

In this study, dynamic quenching of the phosphorescence of Pt porphyrins by a series of 2P dyes was used to evaluate relative efficiencies of photoinduced ET's in the chromophore pairs. The ET driving forces were correlated with the phosphorescence quenching rate constants in order to establish that ET is the main quenching pathway [31,35].

3.2. Triplet chromophores

A series of phosphorescent Pt(II) *meso*-tetraarylporphyrins with redox potentials varying in a wide range was selected (Fig. 1). Pt porphyrins exhibit strong room temperature phosphorescence with lifetimes τ_0 in the range of 40–60 μs (see Table 1).

Porphyrins shown in Fig. 1 form two structurally different groups: "regular" Pt tetraarylporphyrins (PtP's, **1**–**8**) and Pt tetraaryltetrabenzoporphyrins (PtTBP's, **9**–**11**). Spectral characteristics within each group vary only slightly, whereas between the groups there are large differences (Fig. 2). Due to the extended π-conjugation, the lowest energy absorption bands (S_0–S_1, Q-bands) of PtTBP's (**9**–**11**) are about 100 nm red-shifted relative to those of PtP's (**1**–**8**). Accordingly, T_1–S_0 phosphorescent bands of PtTBP's also have lower energies; and this might result in lower driving forces for ET's involving PtTBP triplet states. Notably, PtTBP's possess higher 2PA cross-sections than PtP's [36,6], which potentially makes them more suitable for 2P applications.

First oxidation and reduction potentials were measured using cyclic voltammetry (see Supplementary Material for examples). In some cases (**1**–**3**, **5**), the first oxidation potentials were beyond the positive potential limit of DMF (0.8 V *vs.* Fc/Fc^+ or 1.30 V *vs.* SCE), while for other porphyrins (**4**, **4a**), the first oxidation was within the potential limit of the solvent, but the current–voltage curve was ill-defined due to a coupled chemical reaction of the electrooxidized species with the solvent. In the latter case, the values for the peak potentials (E_{pa}) are listed for the scan rate of 0.1 V/s. Notably, similar potentials were measured in PhCN and were reversible by both cyclic voltammetry and thin-layer spectroelectrochemistry. For this reason, the E_{pa} values in DMF are assured to be close to $E_{1/2}$ values in PhCN.

The first reduction of each porphyrin is reversible and well defined in DMF. Importantly, the ring reduction potentials shift negatively with a decrease in the electron-withdrawing character of the substituents in the *meso*-aryl rings. The same shift in the potential was observed upon oxidation (or reduction), and the electrochemically measured separation between the potentials for the first ring-centered oxidation and the first ring-centered reduction was constant for all PtP's.

3.3. 2P dyes

The following characteristics were considered when selecting 2P dyes: (i) strong fluorescence, overlapping with absorption of Pt porphyrins for maximally efficient FRET; (ii) strong 2P absorption, shifted maximally to the red relative to the phosphorescence of Pt porphyrins in order to avoid possible interference of linear absorption *via* direct $S_0 \rightarrow T_1$ mechanism [37,6]; (iii) synthetic availability and ease of functionalization.

Absorption Q-bands of PtP's (**1**–**8**) are situated between 500 and 540 nm (Table 1). Unfortunately, the choice of suitable 2P absorbers emitting in this wavelength range was limited, mostly because many of them exhibit strong solvatochromism [38]. These dyes flu-

Table 1
Selected photophysical and electrochemical properties of Pt porphyrins used in this study

#	λ_{abs}(Q) (nm)[a]	λ_{phos} (nm)[a]	ϕ_{phos}[a,b]	τ_0 (μs)	E_{00} (eV)[c]	E^1_{ox} (V)[a,d]	E^1_{red} (V)[a,d]
1	512, 542	662, 727	0.1	56	1.87	[e]	−1.35
2	512, 540	663, 730	0.07	32	1.87	[e]	−1.53
3	509 539	669, 732	0.07	52	1.85	[e]	−1.65
4, **4a**	509 539	663, 727	0.09	55, 48	1.87	0.86[f]	−1.66
5	510, 539	671, 731	0.05	34	1.85	[e]	−1.68
6, **6a**	511, 540	683, 742	0.07	38, 39	1.81	0.79	−1.68
7, **7a**	510, 540	662, 730	0.11	76, 79	1.87	0.70	−1.91
8	510, 540	668,732	0.11	74	1.86	0.67	−1.94
9	617	783	0.10	29	1.58	0.37	−1.61
10	620	787	0.15	45	1.57	0.50	−1.55
11	624	767	0.07	14	1.62	0.60	−1.23

[a] In DMF.
[b] Rhodamine B in MeOH was used as the standard ($\phi_{fluo} = 0.5$) [26,27].
[c] E_{00} was calculated from the blue edge of the lowest vibrational band ($T_{10} \rightarrow S_{00}$) in the phosphorescence spectrum.
[d] *vs.* Fc/Fc^+ (0.50 V *vs.* SCE in DMF).
[e] The oxidation potentials are beyond the positive limit of DMF.
[f] Current–voltage curve was ill-defined due to a coupled reaction of the electrooxidized species with the solvent.

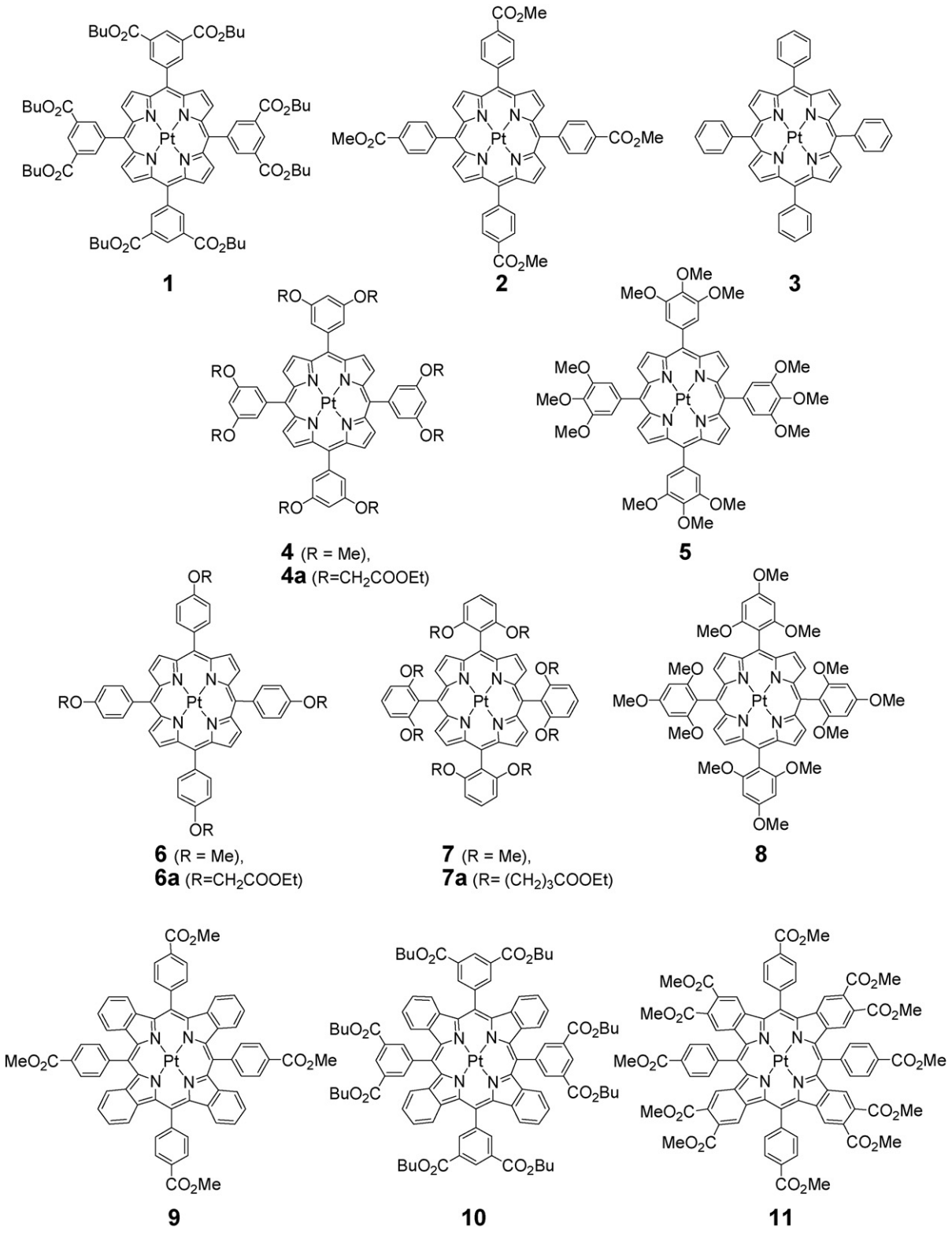

Fig. 1. Pt porphyrins used as triplet chromophores in dynamic quenching experiments.

oresce near 500 nm in non-polar media, e.g. in toluene, but in polar solvents, their emission may shift by as much as several hundred nanometers. Such strong shifts would inevitably lead to significant losses in the FRET efficiency, and that would decrease performance of the sensors, designed to operate in biological aqueous environments.

Research in the area of 2P chromophores is mostly focused on their optical properties, whereas their electrochemical potentials are rarely known. A few exceptions include well-known fluorophores, such as rhodamine B [39] and several recently developed dyes, whose redox potentials were examined in order to explain their 2PA behavior [38b].

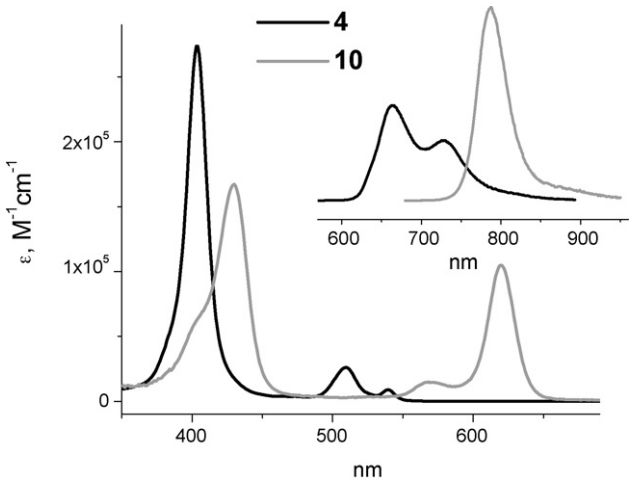

Fig. 2. Absorption and phosphorescence (inset) spectra of representatives of two groups of Pt porphyrins: PtP **4** and PtTBP **10**, in DMF. Emission was excited at 510 nm (**4**) and 615 nm (**10**).

In the absence of detailed data on solvatochromism and redox behavior, the 2PA antennae chromophores were chosen to represent basic classes of 2PA dyes. The selected molecules are shown in Fig. 3 and their absorption and emission spectra are shown in Fig. 4.

Dyes **A**–**E** fluoresce in the region of 480–550 nm (Fig. 4B) and exhibit good spectral overlap with the Q-bands of PtP's (**1**–**8**) in polar solvents (e.g. DMF, see Table 2). Dye **A**, known as AF-50, is a well-characterized 2PA chromophore, a member of a class of 2PA dyes developed in the Air Force research laboratories [40]. Dyes **B**–**D** represent a class of push–pull stilbenoids. The derivative of coumarin-343 (C343), dye **E**, although a relatively weak 2P absorber (σ_2 = 28 GM at 840 nm) (Table 2), was chosen for its high quantum yield, efficient FRET onto PtP's [1], availability and ease of functionalization. Importantly, **E** is a relatively small molecule, which makes it feasible to incorporate several C343 units into a single probe molecule without perturbing its overall structure and solubility.

Both the oxidation and reduction of most 2P dyes (except for the reduction of **F**) were irreversible on the electrochemical time-scale. Therefore, the peak potentials E_{pa} and E_{pc} (listed in Table 2) were used as approximations for the positions of the true oxidation and reduction potentials for the purpose of the Rehm–Weller formula. The reduction potentials of dyes **A**–**E** are significantly lower than those of Pt porphyrins, which is consistent with the expectation that dyes **A**–**E** quench the phosphorescence of Pt porphyrins *via* the reductive mechanism.

The derivative of rhodamine B, dye **F**, is an effective FRET donor for PtTBP's [6]. The first oxidation potential of **F** (E_{ox} = 0.64 V) is substantially higher than the potentials of all the other dyes (Table 2), while its reduction potential (E_{red} = −1.21 V) suggests that **F** is likely to play the role of the oxidant in photoinduced ET reactions with PtTBP's. The 2PA maximum of RhB is located at 840 nm (σ_2 = 210 GM) [29,30]. It is known that excitation of RhB–PtTBP assemblies at 840 nm can lead to linear excitation of PtTBP's due to the presence of relatively strong direct S_0–T_1 absorption bands in their spectra [6]; but it is feasible to use RhB-donors with porphyrins, whose triplet bands do not interfere with excitation at 840 nm.

3.4. Dynamic quenching experiments

Phosphorescence lifetimes were used to monitor quenching of porphyrin triplet states by 2P dyes. Using lifetimes, as

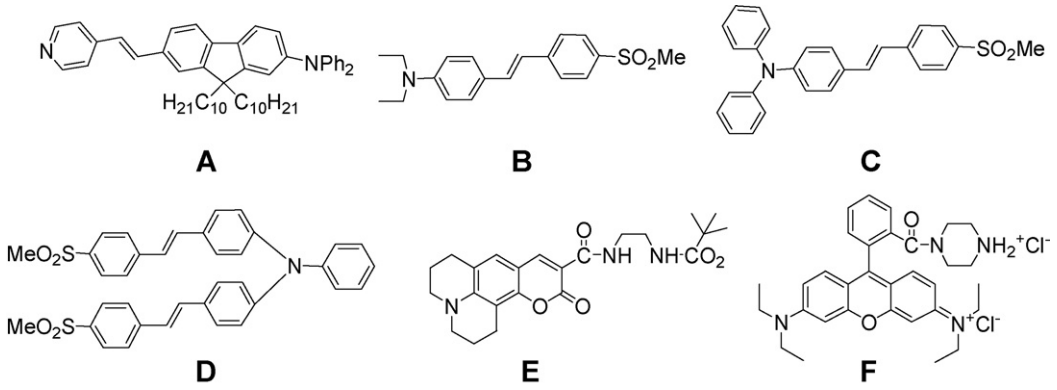

Fig. 3. 2PA dyes used as quenchers in dynamic quenching experiments.

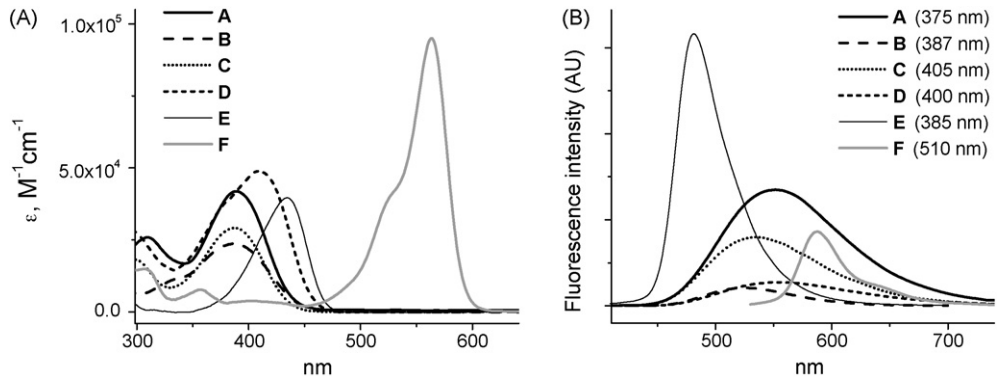

Fig. 4. Linear absorption (A) and fluorescence (B) spectra of 2PA dyes. The emission spectra are scaled to represent the relative emission quantum yields. The excitation wavelengths for each dye are shown in parentheses next to the labels.

Table 2
Properties of two-photon absorbing dyes

#	λ_{abs} (nm)[a] ($\log\varepsilon$)	λ_{fluo} (nm)[a]	ϕ_{fluo}[a,b]	λ_{2PA} (nm)	σ_2 [ref] (GM)[c]	E^1_{ox} (V)[a,d]	E^1_{red} (V)[a,d]
A	387 (4.63)	552	0.9	840	55[e] [41]	0.43	−2.28
B	388 (4.38)	520	0.1	800	~10 [40b]	0.23	[f]
C	386 (4.47)	537	0.5	770	90 [23]	0.47	−2.30
				750	50 [42]		
				840	45[e]		
D	410 (4.69)	552	0.2	815	195 [23]	0.47	−2.34
				840	110[e]		
E	434 (4.60)	480	1.0	840	28[e]	0.51	−2.09
F	564 (4.98)	587	0.2	840	210 [29]	0.64	−1.21[f]

[a] In DMF.
[b] Rhodamine B in MeOH was used as a standard (ϕ_{fluo} = 0.5) [26,27].
[c] 1 GM = 10^{-50} cm^4 s photon^{-1}.
[d] Measured *vs.* Fc/Fc$^+$(0.50 V *vs.* SCE in DMF). Irreversible waves were observed; the corresponding peak potentials E_{pa} and E_{pc} are shown instead of midpoint potentials.
[e] Measured in this work in femtosecond regime using relative fluorescence method with rhodamine B in MeOH as a standard. See Supporting Information for details.
[f] The reduction potential was beyond the negative limit of DMF.

opposed to intensities, makes it easier to discriminate between static and dynamic quenching and exclude static quenching artifacts [10,14]. The general procedure in our experiments involved titration of dilute solutions of Pt porphyrins with 2PA dyes in *N*,*N*-dimethylformamide in the absence of oxygen. Phosphorescence lifetimes were measured as a function of the dye concentration, and quenching constants k_q were calculated as slopes of the Stern–Volmer quenching plots.

Selected Stern–Volmer plots are shown in Fig. 5, and the values of the corresponding quenching constants are given in Table 3. The first graph (Fig. 5A) illustrates quenching of the phosphorescence of a representative PtP, Pt(II) *meso*-tetraphenylporphyrin (PtTPP, **3**), by 2P dyes **A**–**E**. Among these dyes, stilbene **B** is the strongest quencher and C343-derivative **E** is the weakest quencher. This trend holds true for most of the PtP's (**1**–**8**) in the series. Dyes **A**–**E** practically do not quench phosphorescence of PtTBP's (Table 3).

Assuming that photoinduced ET is the main quenching process, such difference in the quenching behavior of PtP's *vs.* PtTBP's can be rationalized by considering the effects of π-conjugation on the electronic structure of porphyrins. PtTBP's (**9**–**10**) have lower oxidation potentials E^1_{ox} and lower excitation energies E_{00} : E^1_{ox}(PtP) > E^1_{ox}(PtTBP), E_{00}(PtP) > E_{00}(PtTBP) (Table 1) [43]. The latter is believed to be caused by destabilization of one of the porphyrin HOMO's and a decrease in the degree of the states mixing

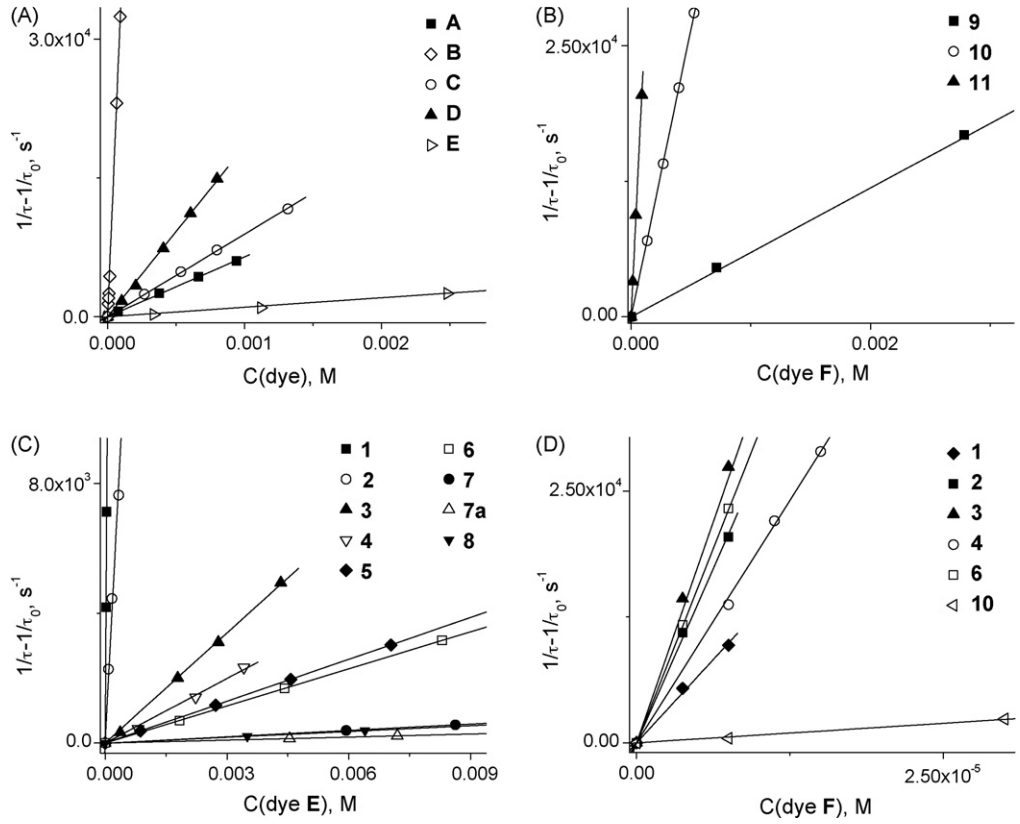

Fig. 5. Selected Stern–Volmer quenching plots. In all the experiments, concentration of Pt porphyrins was about 10^{-6} to 10^{-5} M. (A) Quenching of phosphorescence of PtP (**3**) by dyes **A**–**F**; (B) quenching of phosphorescence of PtTBP's (**9**–**11**) by dye **F**; (C) quenching of phosphorescence of PtP's (**1**–**8**) by dye **E**; (D) quenching of phosphorescence of PtP's **1**–**6** and PtTBP (**10**) by dye **F**.

Table 3
Rate constants[a] k_q ($M^{-1}\,s^{-1}$) for dynamic quenching of phosphorescence of Pt porphyrins by 2PA dyes **A**–**F** in DMF

Pt porphyrin	2PA dye					
	A	**B**	**C**	**D**	**E**	**F**
1	4.4×10^8	1.4×10^9	5.5×10^7	1.9×10^8	1.9×10^8	1.3×10^9
2	2.3×10^7	1.6×10^9	1.3×10^7	2.7×10^7	2.1×10^7	2.7×10^9
3	6.5×10^6	3.6×10^8	7.4×10^6	1.6×10^7	1.0×10^6	3.5×10^9
4	2.8×10^6	4.2×10^8	–	1.8×10^7	6.6×10^5	1.9×10^9
5	–	–	3.9×10^6	7.5×10^6	3.7×10^5	–
6	1.7×10^6	8.8×10^7	2.9×10^6	5.7×10^6	4.7×10^5	3.1×10^9
7(**7a**)	8.8×10^5	9.3×10^6	1.8×10^6	5.3×10^6	6.5×10^4 (3.1×10^4)	–
8[b]	–	7.5×10^6	–	–	6.0×10^4	–
9	0	0	0	0	0	2.3×10^8
10	0	0	0	0	0	5.3×10^7
11[c]	–	–	–	–	0	5.5×10^6

[a] Each k_q value was derived as the average from three independent experiments. k_q values from different experiments varied within about 10% of the average.
[b] The quenching rates for porphyrin **8** and dyes **A**, **C** and **D** were not measured because these quenching experiments required very large amounts of the 2P dyes. On the other hand, dye **B** was found to be the strongest quencher for all the other PtP's, whereas dye **E** was the weakest for the PtP's with lower reduction potentials (**3**–**7**). By extrapolation, k_qs for the pairs **8**/**B** and **8**/**E** provide the upper and the lower limits for the quenching rate constants of **8** by all the other dyes.
[c] Phosphorescence of PtTBP **11** is quenched by dyes **A**–**D** very weakly.

for TBP's [43b,c]. The decrease in the oxidation potential of TBP's *vs.* regular porphyrins is also associated with the higher energy of the HOMO. The first reduction E^1_{red} potentials of PtTBP's and PtP's, however, are quite close: $E^1_{red}(PtP) \approx E^1_{red}(PtTBP)$.

When Pt porphyrins participate as donors in the ET with the same dye (Fig. 6A—oxidative quenching), the differences between the driving forces for similarly substituted PtP and PtTBP are expected to be small, provided the differences in E_{00}'s and E^1_{ox}'s are close ($E_{00}(PtP) - E_{00}(PtTBP) \approx E^1_{ox}(PtP) - E^1_{ox}(PtTBP)$) and cancel out in the Rehm–Weller formula (Eq. (2)). On the other hand, if porphyrins play the role of acceptors (Fig. 6B—reductive quenching), the ET driving forces should be lower for PtTBP's than for PtP's because $E^1_{red}(PtTBP) \approx E^1_{red}(PtP)$ and $E_{00}(PtTBP) < E_{00}(PtP)$.

Interestingly, while it is expected that the quenching rates for PtP's and PtTBP's by the oxidative mechanism (dye **F**) should be close, the measured constants k_q for the PtP's appear to be much higher than those for PtTBP's and do not correlate with the PtP's redox potentials. This behavior suggests the presence of another efficient quenching process, which is likely to be the triplet–triplet energy transfer in RhB/PtP pairs. The T_1–S_0 energy gaps in PtP's (**1**–**8**) and in RhB are quite close, i.e. 1.82–1.87 eV (662–680 nm, see Table 1) and 1.86 eV (667 nm) [44], respectively, making the triplet energy transfer feasible.

Within the PtP and PtTBP subsets, E_{00} values remain practically constant, and the ET driving forces change in parallel with the porphyrin's oxidation or reduction potentials, depending on the ET direction. Graphs in Fig. 5B and C illustrate the effects of porphyrin redox potentials on the quenching rates in the two series: (B) PtTBP's—oxidative quenching by dye **F**; and (C) PtP's—reductive quenching by dye **E**. Plots in graph C reflect the fact that k_q values correlate with reduction potentials (E^1_{red}) of PtP's, and the most electron-rich porphyrins **6**–**8** are the least susceptible to quenching. For PtTBP's (**9**–**11**) (graph B), dye **F** performs as the oxidant; and, consequently, constants k_q correlate with the oxidation potentials (E^1_{ox}). It should be mentioned that T_1–S_0 energy gaps in PtTBP's are about 1.6 eV, making RhB ← PtTBP triplet–triplet exchange unfavorable and leaving the ET the predominant quenching pathway.

The obtained data show that in the PtP-series quenching by the ET is minimal when the electron-rich porphyrins (e.g. **6**–**8**) are paired with C343-derivative **E**. The observed rate constants are lower by as much as 10^5 times than those obtained for combinations of, e.g. porphyrin **1**, bearing eight electron-withdrawing carboxyl groups, with strongly reducing dyes such as **B**. Considering availability of **E** and its relatively small size, this coumarin-based chromophore will likely to be the primary choice for the construction of 2P-enhanced phosphorescent probes.

3.5. Kinetic model and correlation of quenching rates with ET driving forces

In order to obtain evidence that the observed phosphorescence quenching was due to the ET, we correlated the values of experimental quenching constants k_q with the driving forces, calculated using the Rehm–Weller formula.

Dynamic quenching of phosphorescence of Pt porphyrins by electro-active quenchers can be described as a sequence of the reactions in Scheme 1.

In Scheme 1, P is Pt porphyrin in its ground state; $^3P^*$ is Pt porphyrin in its excited triplet state; ($^3P^*\cdots Q$) and ($P^{-}\cdots Q^{+}$) refer to the encounter complex before and after the ET step, respectively;

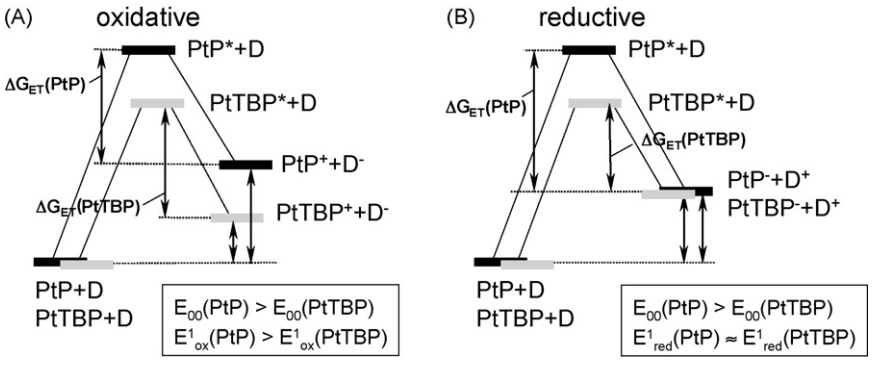

Fig. 6. Energy diagrams for oxidative (A) and reductive (B) quenching of phosphorescence by ET.

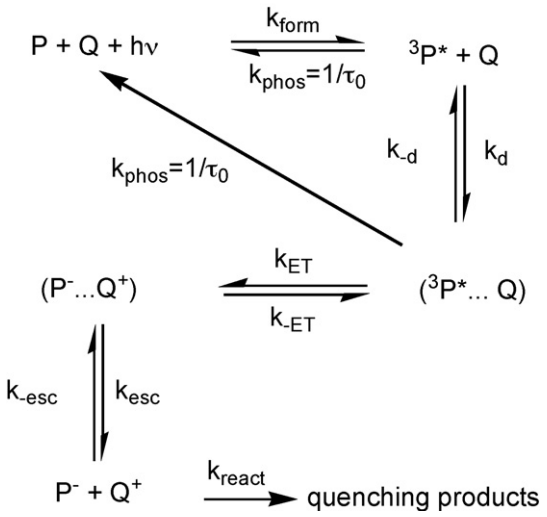

Scheme 1.

P^- and Q^+ refer to the ionic products of the ET reaction after their escape from the solvent cage. k_{form} refers to the combined rate of formation of the triplet state $^3P^*$, which includes the rates of absorption, fluorescence, internal conversion of the singlet state and intersystem crossing. Rate constant k_{phos} is the actual rate of disappearance of the triplet state measured by the phosphorescence emission. This constant accounts for both the radiative and non-radiate decays to the ground state. Constants k_d (k_{-d}), k_{ET} (k_{-ET}) and k_{esc} (k_{-esc}) refer to the diffusion, electron transfer and cage escape processes and their inverses, respectively; and constant k_{react} refers to irreversible reaction(s) involving the ionic species P^- and Q^+. It should be mentioned that in Pt and Pd porphyrins, rates of intersystem crossing are usually very high [45,37], and triplet states are formed with practically unity quantum yields [46].

Formal treatment yields the following expression for quenching constant k_q (for detailed derivation see Supporting Information):

$$k_q = \frac{k_d k_{ET} k_{esc}}{(k_{-d} + 1/\tau_0 + k_d[Q])[k_{-ET}(1 + (k_{-esc}/k_{react})) \quad + k_{esc}(1 + (k_{ET}/(k_{-d} + 1/\tau_0 + k_d[Q])))]} \tag{3}$$

We further assume that (i) no significant interaction between the reagents occurs in the encounter complex ($^3P^*\cdots Q$), i.e. $k_{-d} \approx k_d$, which is suggested by the fact that the emission spectra of the mixtures containing 2P dyes are identical to those of pure Pt porphyrins; (ii) the diffusion is much faster than the emission of phosphorescence, i.e. $k_d \gg k_{phos}$; and (iii) the rate of the cage escape is much lower than the rate of the formation of the final products, i.e. $k_{-esc}/k_{react} \ll 1$. Combining assumptions (i) and (ii) into $k_{-d} \gg 1/\tau_0 + k_d[Q]$ at low quencher concentrations ($Q \ll 1$), Eq. (3) can be rewritten as [47]:

$$k_q = \frac{k_d}{1 + k_{-d}/k_{ET} + k_{-d}k_{-ET}/k_{esc}k_{ET}} = \frac{k_d}{1 + [k_{-d}/(k_e^0 \exp(-\Delta G_{ET}^*/RT))] + (k_{-d}/k_{esc})\exp(\Delta G_{ET}/RT)} \tag{4}$$

In the last formula, k_{ET} was expressed as $[k_e^0 \exp(-\Delta G_{ET}^*/RT)]$ from the Arrhenius equation; and k_{-ET}/k_{ET}, which is the reciprocal of the electron transfer equilibrium constant (K_{ET}), was substituted for $[\exp(\Delta G_{ET}/RT)]$. Here k_e^0 is the frequency factor, ΔG_{ET}^* is the free energy of activation for the ET step, and ΔG_{ET} is the driving force of the ET reaction. ΔG_{ET}^* can be further expressed using the Marcus–Hush theory [33] in terms of ΔG_{ET} and reorganization energy λ:

$$\Delta G_{ET}^* = \frac{(\Delta G_{ET} + \lambda)^2}{4\lambda} \tag{5}$$

Experimentally determined k_q's and their decimal logarithms ($\log k_q$) were plotted against the corresponding driving forces ΔG_{ET} (Fig. 7). In calculation of ΔG_{ET} we omitted the work terms w. In polar solvents Coulombic interactions in the ion pairs are typically expected to be small [48]. In addition, it is likely that the work terms were similar in the dye pairs studied (except for some cases, see below) and, therefore, they could be omitted for the purpose of our comparison. As expected, all the dependencies of $\log k_q$ on ΔG_{ET} were linear through the most of the range; and for the quenching of phosphorescence of PtP's (**1**–**8**) by the most reducing dye **B** (Fig. 7A) the plot began deviating from linearity. These data support the assumption that the phosphorescence quenching in our experiments was indeed caused by the ET [17], and the comparisons drawn in Section 3.4 were appropriate.

Interestingly, in the cases involving large hydrophobic dyes (**A**, **C**, and **D**) in combination with porphyrins **7** and **8**, bearing substituents in 2,6-positions of their *meso*-aryl rings, the observed quenching rates were higher than expected from the Marcus plots

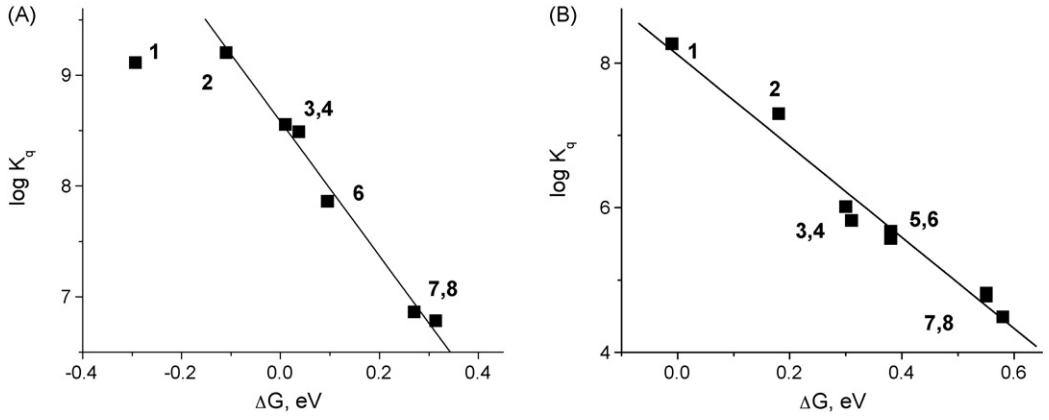

Fig. 7. Decimal logarithms of experimental constants k_q for quenching of phosphorescence of PtP's (**1**–**8**) by dye **B** (A) and dye **E** (B), plotted against the driving force of photoinduced ET (ΔG_{ET}).

based on the other dye pairs. It is possible that in these cases the higher rates were caused by lower work terms w, since the effective separation between the ions in the corresponding ion pairs was larger due to the steric reasons. In addition, the geometry of the encounter complexes involving bulky dyes and 2,6-substituted PtP's could be different, affecting the reorganization energy. In principle, fitting experimental points to the function given by Eq. (3) should produce kinetic parameters k_d, k_{-d}/k_e^0, $\Delta G_{ET}^*(0)$, k_{-d}/k_{esc}, as well as the reorganization energy λ [47]. However, such fitting in practice would be highly unstable because of the large number of parameters, their implicit dependence and noise in the data.

4. Conclusion

The results of this study demonstrate that dynamic quenching of phosphorescence is a simple and effective screening method for selecting pairs of FRET donors and FRET acceptors for construction of 2P-enhanced triplet devices. Several conclusions from this work are summarized below.

First, most 2PA dyes studied in this work (**A**–**E**) act as strong reducing agents with respect to Pt porphyrin triplet states. Dyes **A**–**E** were selected as representatives of larger classes of structurally related chromophores, i.e. neutral push–pull stilbenoids with various degrees of conjugation. If such dyes are to be used as 2P antennae, they would have to be paired with porphyrins (or other triplet chromophores) with lowest possible reduction potentials to avoid quenching.

Secondly, based on the data for dyes **A**–**D**, which belong to the class of push–pull (D-π-A) dyes [38b], predictions can be made for structurally related chromophores by taking into account how they differ in donor/acceptor character and degree of conjugation. For example, it can be inferred that (1) all D-π-D dyes containing diphenylamino groups or stronger donors will reduce triplet states of PtP's; (2) D-π-A dyes similar to the studied ones in donor character (i.e. containing same or stronger donor groups) would quench PtP, but not PtTBP, triplet states.

Thirdly, in spite of the fact that all PtP's (**1**–**8**) were to some extent quenched by all the dyes studied, the ET rates varied by as much as 10^5 times from the most strongly quenched to the most weakly quenched pair. Lowering the excited state energy (E_{00}) by varying porphyrin structure, e.g. as in the case of π-extended PtTBP's (**9**–**11**), points toward the possibility to decrease reductive quenching of triplet states. For example, partially extended porphyrins (mono-, di- and tribenzoporphyrins) should be more difficult to reduce compared to regular PtP's.

Finally, for electron-rich PtP's, such as **6**–**8**, rates of quenching by **E** were found to be very small ($\sim 10^4$ to 10^5 M^{-1} s^{-1}), suggesting that in covalent assemblies, where ET can be additionally attenuated by spatial separation, these pairs of chromophores should exhibit superior performance.

Acknowledgements

Support of the grants EB007279 and HL081273 from the NIH USA is gratefully acknowledged. We thank Dr. L.-S. Tan (AFRL/MLBP) for providing a sample of AF-50.

Appendix A. Supplementary data

Supplementary data associated with this article can be found, in the online version, at doi:10.1016/j.jphotochem.2008.02.020.

References

[1] R.P. Briñas, T. Troxler, R.M. Hochstrasser, S.A. Vinogradov, J. Am. Chem. Soc. 127 (2005) 11851–11862.
[2] (a) A. Karotki, M. Kruk, M. Drobizhev, A. Rebane, E. Nickel, C.W. Spangler, IEEE J. Sel. Top. Quant. Electron. 7 (2001) 971–975;
(b) M. Drobizhev, A. Karotki, M. Kruk, N.Z. Mamardashvili, A. Rebane, Chem. Phys. Lett. 361 (2002) 504–512.
[3] (a) W.R. Dichtel, J.M. Serin, C. Edder, J.M.J. Fréchet, M. Matuszewski, L.S. Tan, T.Y. Ohulchanskyy, P.N. Prasad, J. Am. Chem. Soc. 126 (2004) 5380–5381;
(b) M.A. Oar, J.M. Serin, W.R. Dichtel, J.M.J. Fréchet, Chem. Mater. 17 (2005) 2267–2275.
[4] M. Morone, L. Beverina, A. Abbotto, F. Silvestri, E. Collini, C. Ferrante, R. Bozio, G.A. Pagani, Org. Lett. 8 (2006) 2719–2722.
[5] K.D. Belfield, C.C. Corredor, A.R. Morales, M.A. Dessources, F.E. Hernandez, J. Fluoresc. 16 (2006) 105–110.
[6] O.S. Finikova, T. Troxler, A. Senes, W.F. DeGrado, R.M. Hochstrasser, S.A. Vinogradov, J. Phys. Chem. A 111 (2007) 6977–6990.
[7] (a) J.M. Vanderkooi, G. Maniara, T.J. Green, D.F. Wilson, J. Biol. Chem. 262 (1987) 5476–5482;
(b) V. Rozhkov, D. Wilson, S. Vinogradov, Macromolecules 35 (2002) 1991–1993;
(c) I.B. Rietveld, E. Kim, S.A. Vinogradov, Tetrahedron 59 (2003) 3821–3831.
[8] (a) R.L. Goyan, D.T. Cramb, Photochem. Photobiol. 72 (2000) 821–827;
(b) M. Kruk, A. Karotki, M. Drobizhev, V. Kuzmitsky, V. Gael, A. Rebane, J. Lumin. 105 (2003) 45–55;
(c) A. Karotki, M. Khurana, J.R. Lepock, B.C. Wilson, Photochem. Photobiol. 82 (2006) 443–452.
[9] M.R. Eftink, C.A. Ghiron, Anal. Biochem. 114 (1981) 199–227.
[10] S.E. Webber, Photochem. Photobiol. 65 (1997) 33–38.
[11] (a) K. Kalyanasundaram, Photochemistry of Polypyridine and Porphyrin Complexes, Academic Press, London, 1992 (Chapters 3–4);
(b) D.M. Roundhill, Photochemistry and Photophysics of Metal Complexes, Plenum Press, New York, 1994, and references therein.
[12] B.W. Ma, P.I. Djurovich, M.E. Thompson, Coord. Chem. Rev. 249 (2005) 1501–1510.
[13] For examples see:
(a) J.V. Mersol, D.G. Steel, A. Gafni, Biochemistry 30 (1991) 668–675;
(b) B.D. Schlyer, E. Lau, A.H. Maki, Biochemistry 31 (1992) 4375–4383;
(c) S. Beckham, M.P. Cook, L. Karki, M.M. Luchsinger, V.R. Whitlock, Y. Wu, Q.F. Zhang, M.D. Schuh, Arch. Biochem. Biophys. 310 (1994) 440–447;
(d) C.Y. Shen, N.M. Kostic, Inorg. Chem. 35 (1996) 2780–2784;
(e) P. Cioni, G.B. Strambini, J. Am. Chem. Soc. 120 (1998) 11749–11757;
(f) E.V. Sokerina, G.M. Ullmann, G. van Pouderoyen, G.W. Canters, N.M. Kostic, J. Biol. Inorg. Chem. 4 (1999) 111–121;
(g) M.M. Crnogorac, N.M. Kostic, Inorg. Chem. 39 (2000) 5028–5035.
[14] (a) M.R. Eftink, M.C.R. Shastry, Fluorescence Spectroscopy, vol. 278, 1997, pp. 258–286;
(b) S. Roy, in Energetics of Biological Macromolecules, Part D, vol. 379, 2004, pp. 175–187.
[15] J.B. Birks, Photophysics of Aromatic Molecules, Wiley Interscience, London, 1970, and references therein (Chapters 9–11).
[16] (a) A. Weller, Discussions Faraday Soc. 27 (1959) 28–33;
(b) T. Förster, Annalen Der Physik 2 (1948) 55–75.
[17] G.J. Kavarnos, N.J. Turro, Chem. Rev. 86 (1986) 401–449.
[18] (a) J.H. Alstrum-Acevedo, M.K. Brennaman, T.J. Meyer, Inorg. Chem. 44 (2005) 6802–6827;
(b) D.M. Guldi, J. Phys. Chem. B 109 (2005) 11432–11441;
(c) S. Fukuzumi, D.M. Guldi, in: V. Balzani (Ed.), Electron Transfer in Chemistry, vol. 2, Wiley–VCH, Weinheim, 2001 (Chapter 8);
(d) V. Balzani, A. Juris, Coord. Chem. Rev. 211 (2001) 97–115;
(e) D. Gust, T.A. Moore, in: K.M. Kadish, K.M. Smith, R. Guilard (Eds.), The Porphyrin Handbook, vol. 8, Academic Press, New York, 2000 (Chapter 57);
(f) K. Kalyanasundaram, M. Gratzel, Coord. Chem. Rev. 177 (1998) 347–414.
[19] Assuming all the parameters equal, the sensitivity of the excited state towards quenching by diffusing molecules is proportional to the excited state lifetime, and, therefore, it is four to five orders of magnitude higher for phosphorescent than for fluorescent chromophores.
[20] (a) J.W. Buchler, C. Dreher, G. Herget, Liebigs Annalen Der Chemie (1988) 43–54;
(b) J.W. Buchler, K.L. Lay, H. Stoppa, Z. Naturforsch. (B) 35 (1980) 433–438.
[21] J.S. Lindsey, I.C. Schreiman, H.C. Hsu, P.C. Kearney, A.M. Marguerettaz, J. Org. Chem. 52 (1987) 827–836.
[22] O.S. Finikova, A.V. Cheprakov, I.P. Beletskaya, P.J. Carroll, S.A. Vinogradov, J. Org. Chem. 69 (2004) 522–535.
[23] C. Katan, F. Terenziani, O. Mongin, M.H.V. Werts, L. Porres, T. Pons, J. Mertz, S. Tretiak, M. Blanchard-Desce, J. Phys. Chem. A 109 (2005) 3024–3037.
[24] A. Ulman, C.S. Willand, W. Kohler, D.R. Robello, D.J. Williams, L.L. Handley, J. Am. Chem. Soc. 112 (1990) 7083–7090.
[25] T. Nguyen, M.B. Francis, Org. Lett. 5 (2003) 3245–3248.
[26] T. Karstens, K. Kobs, J. Phys. Chem. 84 (1980) 1871–1872.
[27] Several values have been reported in the literature for the fluorescence quantum yield of rhodamine B, ranging from 0.41 to 0.97: J.N. Demas, G.A. Crosby, J. Phys. Chem. 75 (1971) 991. We used the value of 0.5, reported by Karstens and Kobs [26] and confirmed by our own measurements.

[28] S.A. Vinogradov, M.A. Fernandez-Seara, B.W. Dugan, D.F. Wilson, Rev. Sci. Instrum. 72 (2001) 3396–3406.
[29] C. Xu, W.W. Webb, J. Opt. Soc. Am. B: Opt. Phys. 13 (1996) 481–491.
[30] A value about seven times lower was recently reported for σ_2 of rhodamine B by Kauert and co-workers: M. Kauert, P.C. Stoller, M. Frenz, J. Ricka, Opt. Express 14 (2006) 8434–8447.
[31] See Ref. [17], p. 419.
[32] D. Rehm, A. Weller, Isr. J. Chem. 8 (1970) 259.
[33] R.A. Marcus, J. Chem. Phys. 24 (1956) 966–978.
[34] Marcus inverted region is not observed in dynamic quenching (see Ref. [17]).
[35] A more rigorous proof, requiring complete spectroscopic signatures of ionic species formed as a result of the ET reaction, was left for the next stage, when the covalent assemblies are constructed from the selected chromophores.
[36] A. Karotki, M. Drobizhev, M. Kruk, C. Spangler, E. Nickel, N. Mamardashvili, A. Rebane, J. Opt. Soc. Am. B: Opt. Phys. 20 (2003) 321–332.
[37] V.N. Knyukshto, A.M. Shul'ga, E.I. Sagun, E.I. Zen'kevich, Opt. Spectrosc. 100 (2006) 590–601.
[38] For example see:
(a) U. Narang, C.F. Zhao, J.D. Bhawalkar, F.V. Bright, P.N. Prasad, J. Phys. Chem. 100 (1996) 4521–4525;
(b) S.J.K. Pond, M. Rumi, M.D. Levin, T.C. Parker, D. Beljonne, M.W. Day, J.L. Bredas, S.R. Marder, J.W. Perry, J. Phys. Chem. A 106 (2002) 11470–11480;
(c) F. Terenziani, A. Painelli, C. Katan, M. Charlot, M. Blanchard-Desce, J. Am. Chem. Soc. 128 (2006) 15742–15755;
(d) K.D. Belfield, M.V. Bondar, O.D. Kachkovsky, O.V. Przhonska, S. Yao, J. Lumin. 126 (2007) 14–20.
[39] A.B. Fischer, I.I. Bronstein-Bonte, J. Photochem. 30 (1985) 475–485.
[40] (a) B.A. Reinhardt, L.L. Brott, S.J. Clarson, A.G. Dillard, J.C. Bhatt, R. Kannan, L.X. Yuan, G.S. He, P.N. Prasad, Chem. Mater. 10 (1998) 1863–1874;
(b) G.S. He, L.X. Yuan, N. Cheng, J.D. Bhawalkar, P.N. Prasad, L.L. Brott, S.J. Clarson, B.A. Reinhardt, J. Opt. Soc. Am. B: Opt. Phys. 14 (1997) 1079–1087.
[41] Literature values for 2PA cross-section of AF-50 vary greatly. In an early work, the value as high as 11,500 GM was reported (Ref. [40a]). More recently measured values are in the range 30–50 GM:
(a) D.Y. Kim, T.K. Alm, J.H. Kwon, D. Kim, T. Ikeue, N. Aratani, A. Osuka, M. Shigeiwa, S. Maeda, J. Phys. Chem. A 109 (2005) 2996–2999;
(b) S. Saita, T. Yamaguchi, T. Kawai, M. Irie, ChemPhysChem 6 (2005) 2300–2306.
[42] T.C. Lin, G.S. He, P.N. Prasad, L.S. Tan, J. Mater. Chem. 14 (2004) 982–991.
[43] (a) M. Gouterman, J. Mol. Spectrosc. 6 (1961) 138–163;
(b) K.A. Nguyen, R. Pachter, J. Chem. Phys. 114 (2001) 10757–10767;
(c) A. Rosa, G. Ricciardi, E.J. Baerends, S.J.A. van Gisbergen, J. Phys. Chem. A 105 (2001) 3311–3327;
(d) K.M. Kadish, O.S. Finikova, E. Espinosa, C.P. Gros, G. De Stefano, A.V. Cheprakov, I.P. Beletskaya, R. Guilard, J. Porph. Phthal. 8 (2004) 1062–1066.
[44] E. Vuorimaa, H. Lemmetyinen, M. VanderAuweraer, F.C. DeSchryver, Thin Solid Films 268 (1995) 114–120.
[45] (a) D. Eastwood, M. Gouterman, J. Mol. Spectrosc. 35 (1970) 359–375;
(b) D.H. Kim, D. Holten, M. Gouterman, J.W. Buchler, J. Am. Chem. Soc. 106 (1984) 4015–4017.
[46] J.E. Rogers, K.A. Nguyen, D.C. Hufnagle, D.G. McLean, W.J. Su, K.M. Gossett, A.R. Burke, S.A. Vinogradov, R. Pachter, P.A. Fleitz, J. Phys. Chem. A 107 (2003) 11331–11339.
[47] I. Mackay, L.Z. Cai, A.D. Kirk, A. McAuley, Inorg. Chem. 38 (1999) 3628–3633.
[48] See Ref. [17], p. 418.